Article Summary Line: Imposing mask usage requirements, group size restrictions, duration limits, and social distancing policies can have additive, and in some cases multiplicative protective effects on SARS-CoV-2 infection risk during indoor events.

Running Title: Indoor SARS-CoV-2 Transmission Interventions

Keywords: aerosol, airborne, agent-based model, COVID-19, coronavirus, droplet, indoor transmission, respiratory pathogen, SARS-CoV-2

Title: Assessing the efficacy of interventions to control indoor SARS-Cov-2 transmission: an agent-based modeling approach

Authors: Trevor S. Farthing, and Cristina Lanzas*

Affiliations: North Carolina State University, Raleigh, North Carolina, USA (T. Farthing, C. Lanzas)

*Correspondence to Cristina Lanzas; clanzas@ncsu.edu

Abstract – 149 words

Intervention strategies for minimizing indoor SARS-CoV-2 transmission are often based on anecdotal evidence because there is little evidence-based research to support them. We developed a spatially-explicit agent-based model for simulating indoor respiratory pathogen transmission, and used it to compare effects of four interventions on reducing individual-level SARS-CoV-2 transmission risk by simulating a well-known case study. We found that imposing movement restrictions and efficacious mask usage appear to have the greatest effects on reducing infection risk, but multiple concurrent interventions are required to minimize the proportion of susceptible individuals infected. Social distancing had little effect on reducing transmission if

24 individuals move during the gathering. Furthermore, our results suggest that there is potential for
25 ventilation airflow to expose susceptible people to aerosolized pathogens even if they are
26 relatively far from infectious individuals. Maximizing rates of aerosol removal is the key to
27 successful transmission-risk reduction when using ventilation systems as intervention tools.
28
29 **Main Text – 3499 words**
30 *1. Introduction*
31 Understanding transmission mechanisms is necessary to generate evidence-based guidance
32 for controlling infectious diseases. Severe Acute Respiratory Syndrome Coronavirus 2 (SARS-
33 CoV-2), the causative agent of Coronavirus Disease 2019 (COVID-19), is primarily spread
34 through infectious respiratory droplets and aerosols of varying size (*1, 2, 3, 4, 5*). These media
35 are expelled when an individual speaks, coughs, sneezes, or otherwise expectorates (*6, 7*).
36 Pathogen transmission can occur when these virion-containing particles are inhaled by, or
37 otherwise come into contact with the mucosae or conjunctiva (i.e., mouth, nasal membranes, or
38 eyes) of a susceptible person (*5*). Aerosol transmission is emerging as an important transmission
39 pathway, particularly for large clusters associated with superspreading events (*2, 8, 9, 10*). van
40 Doremalen et al. (2020) (*11*) found that SARS-CoV-2 can remain viable in aerosolized droplets
41 for at least 3 hours post expectoration. While these results may not accurately represent SARS-
42 CoV-2 stability outside of laboratory conditions (*5*), their findings are in line with case reports of
43 viral-RNA detection in air collected from hospital rooms housing COVID-19 patients (*12, 13,*
44 *14, 15*).
45 Transmission of SARS-CoV-2 is more likely in indoor settings than outdoors (*8, 9*).
46 Households are the most common venue linked to transmission, but healthcare facilities,

47 religious venues, food processing plants or prisons are also likely to be associated with large
48 clusters of COVID-19 cases (*9*). Recommended interventions to reduce indoor transmission
49 include: social distancing, use of face coverings, increased ventilation, and reduced group sizes
50 (*1*). U.S. state government recommendations and restrictions for group size limits in indoor
51 gatherings range from 10 to 100 people or 10 – 75% of a locale's original capacity (*16*). There is
52 little evidence-based research to support specific group size restrictions, however, and few
53 studies have sought to identify the most-effective strategy for limiting indoor SARS-CoV-2
54 transmission.

55 Some mathematical models have been built to support individual-level risk assessment of
56 indoor transmission and analyze aerosol contributions to past outbreaks. Chande et al. (2020)
57 (*17*) created a tool to assess the U.S. county level probability that someone infected with SARS-
58 CoV-2 will attend events of varied sizes. Their tool is useful for estimating the probability that
59 SARS-CoV-2 transmission could occur during any gathering, but provides no direct measure of
60 transmission risk from infectious individuals during events and no way to assess the impact of
61 intervention strategies other than reducing group sizes. Other models have sought to determine
62 the role that aerosolized infectious droplets play in indoor SARS transmission relative to larger
63 droplets that are unlikely to be inhaled, and quantify the transmission risk attributable to aerosols
64 in varied environments (*18, 19, 20, 21, 22*). These models are primarily based on Wells-Riley
65 equations for estimating aerosol-attributable risk, which assume homogenous spatiotemporal
66 mixing of air constituents and exposure to infectious agents (*23*). Mathematical indices and
67 parameter values in these models can be adjusted to simulate effects of intervention strategies
68 like social distancing (*22*) and increased ventilation rates (*18, 20, 21, 22*), but are insufficient for
69 capturing or accounting for any behavior- or environment-mediated spatiotemporal heterogeneity

in transmission risk. Shao et al. (2021) (*24*) used a fluid dynamics model to simulate ventilation effects on SARS-CoV-2 transmission while allowing for heterogenous droplet movement behaviors. Their findings highlight the need to account for within-room spatial heterogeneity when studying indoor transmission risk, as phenomena like ventilation can increase infection risk to individuals in one area of a room or building while simultaneously mitigating risk in another.

Here, we present a spatially-explicit agent-based model (ABM) for simulating within-room respiratory pathogen transmission to inform policy-making decisions aiming to mitigate indoor transmission and implementing individual-level interventions. By simulating spatiotemporal droplet dynamics (e.g., emission of varying droplet size and subsequent distribution in the environment) as well as allowing for dynamic movement and positioning of infectious and susceptible individuals, our model allows virion exposure rates to vary within indoor settings. We use our model to estimate effects of proposed COVID-19 intervention strategies for indoor environments (i.e., increased airflow, limiting contact durations, wearing masks, and increased interpersonal spacing). For benchmarking purposes, we simulate the outbreak that took place during a choir practice in Skagit County, WA in March 2020 (*2*). Additionally, we further investigate potential drivers of superspreading events, like the Skagit County example, by characterizing and comparing how different aspects of indoor gatherings (i.e., population density, duration, quanta production by infectious individuals, and ventilation effects) impact transmission risk. Through these analyses we provide guidance for minimizing SARS-CoV-2 transmission during indoor gatherings.

2. Methods

2.1 Model Description

We developed a spatially-explicit, stochastic ABM to simulate both direct-droplet and airborne respiratory pathogen transmission in indoor settings. This model was created and executed using the open-source modeling software, NetLogo (Ver. 6. 1. 1) (*25*) and is available for download at https://github.com/lanzaslab/droplet-ABM. In Appendix S1 we provide a detailed description of our model in accordance with ODD (Overview, Design concepts, Details) standards outlined by (*26*). We present a limited summary of the model design below. When describing infectious media in our model, we use the term "droplet" to refer to respiratory droplets of any size.

Agents in our model represent people congregating in a fixed space (e.g., students in a classroom, diners in a restaurant, etc.). Patches (i.e., grid cells in the NetLogo model interface) represent 1 x 1 m^2 areas, and the spatial extent can range from 1 to ∞ m^2. The model time step is 1 minute. Droplets ranging from 3 to 750 μm in diameter are expelled by infectious agents. Subsequently, droplets can be inhaled, fall out, diffuse to nearby patches, move via directed airflow, and decay at fixed rates over the course of a simulation. Infection in our model is driven by exposure to virions contained in these droplets, and the number of virions per droplet scales with droplet size. The rate at which droplets fall out (i.e., are removed from circulating air flows) of the simulation is based on the calculated terminal velocity falling speed for droplets, and therefore varies with droplet size. Droplet sizes incapable of settling on the ground within one minute are allowed to move between patches via ventilation- and diffusion-induced airflow. Thus, risk of exposure and subsequent infection for susceptible individuals varies by space and time during the simulation (Figure 1). We recognize that the ability of forced air ventilation systems to reduce local respiratory pathogen transmission is linked to their ability to move aerosolized droplets away from susceptible individuals in three dimensions (*18, 24*). Though this

effect is not explicitly tied to airflow inputs in our model, which only allows airflow in two dimensions, we can effectively simulate ventilation-induced aerosolized droplet movement to heights outside of individuals' inhalation ranges by increasing the decay rate when ventilation effects are simulated. In addition to controlling the number of individuals present and the size of the simulated world, users can dictate infectiousness parameters and other scenario-specific variable values (e.g., number of infectious individuals, probability that infectious individuals are asymptomatic, cough frequency, number virions per mL of droplet fluid, risk of infection given exposure to 1 virion, etc.), ventilation parameters (e.g., direction and speed of airflow, droplet filtration probability, etc.), and adherence to transmission-risk-reduction guidelines (e.g., mask usage, local social distancing, etc.).

2.2 Testing SARS-CoV-2 transmission reduction strategies

2.2.1 Case scenario and model inputs

In March 2020, there was a probable SARS-CoV-2 superspreading event during a choir practice taking place at a church in Skagit County, Washington, USA (*2*). Sixty-one people were in attendance, one attendee was experiencing flu-like symptoms at the time and later tested positive for COVID-19 (*2*). This individual likely infected 53 other attendees over the course of the event (*2*). We briefly describe our rationale for setting scenario-specific input values to simulate this case in our model below, but more-detailed explanations for input and parameter values are given in Appendix S2, and Appendix S3 describes how sensitive simulated infection risk is to variations in select model parameters.

We know from (*2*) that the choir practice lasted 150 minutes in total, split into 4 distinct time intervals. In our simulations, we decided to rearrange agents in our model after 40, 90, and 105 minutes to recreate mixing associated with changing time intervals. At timestep 105, individuals

138 moved back to their initial placements, representing their adherence to assigned seating during
139 interval 4 (i.e., minutes 105 – 150). The seating chart has not been shared due to privacy
140 concerns (*21*) however, we can assume that a maximum of 2 people could be within 1-m^2
141 patches in this scenario. We set the inhalation rate for simulated individuals to 0.023 m^3 air/min,
142 a rate consistent with adults participating in light activity (*27*). Because it is uncertain whether or
143 not the forced-air system was turned on during the choir practice (*21*), we decided to run our
144 simulations in two sets: ventilation-on (i.e., both forced-air effects and natural diffusion moved
145 droplets between patches) and ventilation-off (i.e., only natural diffusion moved droplets
146 between patches).

147 In addition to model the baseline scenario, we modulated values of model inputs related to
148 group-level risk-reduction strategies (i.e., limited population, limited contact durations, mask
149 usage, and meter-level social distancing) between simulations in order to assess the efficacy of
150 each strategy on reducing the number of susceptible individuals infected. Regarding mask usage,
151 we assumed face coverings have both source-prevention and wearer-protection effects, and
152 reduced global droplet exposure/exhalation rates by 0%, 25%, 50%, 75% and 90%. The upper
153 range here is intended to simulate the use of N95 and simple surgical masks, which are estimated
154 to reduce aerosol emission rates by approximately 90% and 74%, respectively (*28, 29*). Lower
155 values are intended to simulate the use of single- and multi-layered fabric masks, for which a
156 wide range of aerosol-filtration efficacies have been reported (*30*). When simulating mask usage,
157 we assumed that all individuals were wearing masks and that all masks had the same efficacy.
158 Table 1 outlines the model input values for our superspreading-scenario simulations.

159 *2.2.2 Running simulations and analyses*

We set up a factorial simulation run within the NetLogo BehaviorSpace using our specified input levels. We ran 1000 replicates of all input set combinations, ultimately resulting in 1,080,000 simulations. Simulations were aggregated into a single data set prior to analysis.

We used a beta regression model with a fixed unknown precision parameter, ϕ, (*31*) to estimate effects of interventions on the mean proportion of susceptible individuals infected in our full simulation set, μ. Beta regression models are employed to analyze proportion data (*31, 32*). We chose to use this method because the potential number of infected individuals in each simulation was limited by the simulated group size, which was a predictor variable of interest, and because preliminary analysis suggested that fitting our data to a beta distribution better explained observed variation than other regression models. We therefore determined it was more appropriate to evaluate effect sizes in terms of the relative proportion of susceptible people infected rather than their total number. We fit our data to the model:

$$\begin{aligned}\ln\left(\frac{\mu}{1-\mu}\right) = {} & \beta_0 + \beta_1(\text{Gathering duration}) + \beta_2(\text{Mask use}) + \beta_3(\text{Mask efficacy}) \\ & + \beta_4(\text{Group size}) + \beta_5(\text{Social distancing}) + \beta_6(\text{Ventilation}) + \beta_7(\text{Movement}) \\ & + \beta_8(\text{Mask use} * \text{Group size}) + \beta_9(\text{Mask use} * \text{Social distancing}) \\ & + \beta_{10}(\text{Group size} * \text{Social distancing}) \\ & + \beta_{11}(\text{Mask use} * \text{Group size} * \text{Social distancing}),\end{aligned}$$

where "Gathering duration," "Mask efficacy," and "Group size" are intervention-strategy variables relating to: minutes of simulated interaction between individuals, the efficacy of worn face masks for reducing expectoration and inhalation of infectious droplets, the simulated population size, and attempted meter-level social distancing in each realized simulation, respectively. The variables "Mask use," "Movement," and "Ventilation" are known confounders related to: reduced droplet spread distance from expectorating infectious individuals wearing

masks, the number of times individuals were rearranged within simulations to reflect mixing of event attendees, and movement of infectious aerosols throughout the simulated space due to a forced-air ventilation system, respectively. "Mask use" is a binary variable taking the value of 1 when simulated individuals are masked (i.e., "Mask efficacy" > 0), and 0 when they are not. "Movement" takes any one value within the range of 1-to-4, dependent on "Gathering duration." "Ventilation" is a binary variable taking the value of 1 for simulations in the "ventilation-on" subset, and 0 for those in the "ventilation-off" subset.

Because beta regression procedures assume all dependent variable values fall between 0 and 1, we used the data transformation procedure described by (*33*) to reconstruct our proportion data without these extremities. All analysis and plotting was carried out using functions from the "betareg" R package (*32*) in RStudio (v. 1.1.463) (*34*) running R (v. 3.6.2) (*35*). We calculated a pseudo-R^2 (*31*) to assess goodness of fit for our regression model

2.3 Evaluating drivers of transmission in indoor gatherings

To assess the relative contribution of environmental conditions to SARS-CoV-2 transmission risk, we conducted a sensitivity analysis to ascertain relative effects of population density, gathering duration, quanta production by infectious individuals, and ventilation on SARS-CoV-2 infection risk beyond the conditions tested in the Skagit County case. In addition, we quantified the ability of different ventilation system aspects (i.e., air-change rate, filtration rate, and effective three-dimensional droplet removal rate) to reduce SARS-CoV-2 transmission risk. Table 2 describes the model input values for these indoor-gathering-risk-assessment simulations.

We set up a factorial simulation run within the NetLogo BehaviorSpace using our specified input levels. We ran 1000 replicates of each parameter set combination when the "Forced air" parameter was set to "on" and when it was "off." We ran these sets separately in order to save

computation time as there were many inputs that only changed when forced airflow was simulated. Ultimately, we produced 144,000 "off" simulations, and 20,160,000 "on" simulations. In both sets, we identified simulations when transmission occurred (i.e., simulations where ≥ 1 person was infected), and recorded this occurrence as the binary variable y_i so that

$$y_i = \begin{cases} 1 & \text{if transmission was observed} \\ 0 & \text{if no transmission occurred,} \end{cases}$$

for each realized simulation, i.

We aggregated simulation data into a single data set and carried out a logistic regression analysis to estimate effects of variable inputs on observed differences in the probability of observing ≥ 1 infections. We fit our data to the model:

$$\ln\left(\frac{\Pr(y_i = 1)}{\Pr(y_i = 0)}\right) = \beta_0 + \beta_1(\text{Population density}) + \beta_2(\text{Gathering duration}) +$$

$$\beta_3(\text{Quanta per hour}) + \beta_4(\text{Excess droplet removal rate}) + \beta_5(\text{Air change rate}) +$$

$$\beta_6(\text{Air filtration rate}),$$

where "Population density" is given by $\frac{n}{\text{m}^2}$, and the "Excess droplet removal rate" (%/min) represents the increased removal of aerosols due to ventilation-induced 3-dimensional droplet movement. It is given by the equation: $(\text{Virion decay rate} - 1.05)$. The 1.05 here represents the general SARS-CoV-2 decay rate (i.e., 1.05%/min) as reported by (*11*). Subtracting this baseline value from the simulated Virion decay rate gives us an excess removal rate that we use as a proxy for 3-dimensional droplet removal attributable to forced airflow movement. When no forced airflow is simulated, excess droplet removal, air change, and filtration rates all equal 0. We calculated the Tjur (*36*) pseudo-R^2 for our logistic regression model to assess goodness of fit.

3. Results & Discussion

We presented a stochastic ABM for studying indoor individual-level respiratory pathogen transmission, and used it to demonstrate the potential effectiveness of multiple intervention strategies for reducing SARS-CoV-2 transmission in an indoor group setting mimicking that of a known superspreading event. We were able to effectively recreate the empirical proportion of susceptible individuals likely infected during the Skagit County superspreading event by simulating the gathering without implementing any intervention strategies (Figure 2).

Our beta regression model for estimating intervention efficacy had a pseudo-R^2 of ≈ 0.43. Given the number of stochastic processes in our ABM, the explanatory power of the model is acceptable. Duration limits and efficacious mask usage appear to have the greatest effects on reducing the proportion of susceptible individuals infected, but multiple concurrent interventions are required to minimize the proportion of susceptible individuals infected (Table 3, Figure 3). However, it is important to note that observed proportional differences are more meaningful for relatively large groups than for smaller ones. The effectiveness of limiting the duration of gatherings for reducing the proportion of infected individuals appears to largely result from reducing the confounding movement effect that increases over time, thereby reducing the probability that susceptible individuals will move from uncontaminated space to areas with greater concentrations of infectious aerosols or nearby to infectious individuals where they may be exposed to large virion-containing droplets (Table 3). We show that simply by limiting the time spent rehearsing that night to 40 min, reducing random mixing between attendees by ending the event prior to splitting into disparate groups (*2*), the proportion of people infected could have been reduced by 70 – 88% even without implementing any other intervention strategies. Therefore, imposing movement restrictions could be a more effective intervention than strict duration limits.

We found that mask usage and social distancing interventions are relatively more effective for reducing proportional infection rates in small groups than in large ones. Our findings suggest that in the Skagit County choral case, duration limits with implied movement restrictions and mask usage would have been the most-effective intervention strategies for reducing SARS-CoV-2 infection rates, but multiple interventions would have needed to be deployed simultaneously to reach near-zero rates (i.e., mean rate < 0.5 people / gathering duration). Infection rates generally increased with group size and decreased with mask efficacy, and we found that when movement rates were minimized (i.e., gathering durations ≤ 40) we could minimize infection rates with relatively-low mask efficacy or even no mask usage in some cases. Our results support recent evidence suggesting that even wearing masks with relatively low droplet-filtering abilities around others can help to reduce exposure to infectious agents (*30, 37*). Attempted social distancing up to 3 m had little effect on transmission rates relative to other intervention strategies. That said, because social distancing generally had a greater effect on proportional infection rates when group size was limited to 10 people, and 2-m social distances reduced the mean number of infections in larger groups, we can intuit that the relatively small overall effect of social distancing was likely due to the presence of physical barriers (e.g., edges of the simulated world) or the physical arrangement of nearby individuals impeding agents' attempts to social distance, rather than due to far-reaching droplet spread that makes social distancing irrelevant.

Conclusions regarding social distancing effects are further supported by our logistic regression model results that describe the relative effects of population density, gathering duration, quanta production, and ventilation on the probability of indoor SARS-CoV-2 transmission from a single infectious individual (Table 4). This model had a pseudo-R^2 value of

273 0.25 and demonstrated that among the considered variables, population density was the most-
274 important contributor to SARS-CoV-2 transmission risk. Additionally, increases in gathering
275 duration, infectious aerosol production, and horizontal air movement all escalate the probability
276 that transmission will occur during gatherings, though the effect is much lesser than that of
277 increasing population density. The relatively small effects of quanta production and duration on
278 transmission risk suggest that once individuals are exposed to infectious agents, they are likely to
279 become infected quickly. Thus, minimizing susceptible people's exposure to infectious media is
280 of paramount importance for controlling COVID-19 incidence.

281 Regarding observed effects of ventilation in our beta and logistic regression models, our
282 results suggest that in spite of some evidence that forced-air ventilation systems can reduce risk
283 of respiratory pathogen infection from indoor aerosols (*38, 39*), there is potential for forced
284 airflow to expose susceptible people to aerosolized pathogens even if they are relatively far from
285 infectious individuals, and therefore increase transmission risk. We show that, though filtering
286 re-circulated air can lower transmission risk (Table 4), increasing this effect is unlikely to
287 compensate for the elevated risk attributable to increased horizontal air-change rates (Tables 3 &
288 4). It appears that maximizing rates of three-dimensional aerosol removal is the key to successful
289 transmission-risk reduction when using forced-air ventilation systems as intervention tools. Our
290 results are therefore consistent with the findings of (*18*), who advise that "displacement"
291 ventilation systems, those designed to vertically stratify indoor air by temperature and remove
292 warmer air, are likely able to reduce local SARS-CoV-2 transmission risk. "Mixing" ventilation
293 systems, designed to distribute temperature and aerosols equally throughout the space, are likely
294 insufficient for preventing transmission and may even facilitate it (*18*).

Given our findings, we maintain that in areas where COVID-19 prevalence remains high, holding events associated with relatively-increased mixing rates between individuals (e.g., social gatherings, sporting events, etc.) should be avoided even if attendance rates are presumed to be low. Such events are likely to be associated with SARS-CoV-2 transmission if ≥ 1 infectious individual(s) were to attend, the probability of which increases linearly with group size (*17*). It is important to note however, that though our results provide insight into mechanisms for reducing SARS-COV-2 transmission rates, given the effect that model parameters can have on simulation outcomes (*see* Appendix S3), our findings may not be reasonably extrapolated to accurately predict transmission in scenarios dissimilar from those we modeled here (e.g., ≥ 2 infectious individuals, fewer aerosolized virions produced during expectorations, etc.). Regardless, we can still conclude that imposing mask usage requirements, group size restrictions, duration limits, and social distancing policies have additive, and in some cases multiplicative protective effects on individual-level SARS-CoV-2 infection risk during gatherings, and can be particularly efficacious interventions when deployed simultaneously.

Acknowledgments

This work was partially supported by CDC U01CK000587-01M001 and R35GM134934.

Author Bio

Trevor S. Farthing is a PhD candidate in the Comparative Biomedical Sciences program at North Carolina State University. His work combines ecological and epidemiological analyses with agent-based infectious disease modeling to quantify and compare driving forces of pathogen transmission in varied pathogen-host systems.

Dr. Cristina Lanzas is an Associate Professor of Infectious Disease at North Carolina State University. Her research focuses on the epidemiology and ecology of infectious diseases in

318 animal and human populations. Her work combines data science, epidemiological analysis and
319 mathematical models to study transmission mechanisms, and to identify and design effective
320 control measures to reduce the public health burden associated with infectious diseases.

321 **References**

322 1. United States Center for Disease Control and Prevention [CDC]. (2020) Scientific brief:
323 SARS-CoV-2 and potential airborne transmission. 2020 [cited 2021 Jan 21].
324 https://www.cdc.gov/coronavirus/2019-ncov/more/scientific-brief-sars-cov-2.html.
325 2. Hamner L, Dubbel P, Capron I, Ross A, Jordan A, Lee J, et al. High SARS-CoV-2 attack rate
326 following exposure at a choir practice – Skagit County, Washington, March 2020. Morb
327 Mortal Wkly Rep. 2020; 69:606-610. doi: 10.15585/mmwr.mm6919e6.
328 3. Lu J, Gu J, Li K, Xu C, Su W, Lai Z, et al. COVID-19 outbreak associated with air
329 conditioning in restaurant, Guangzhou, China, 2020. Emerg Infect Dis. 2020; 26(7):1628-
330 1631. doi: 10.3201/eid2607.200764.
331 4. Shen Y, Dong H, Wang Z, Martinez L, Sun Z, Handel A, et al. Community outbreak
332 investigation of SARS-CoV-2 transmission among bus riders in eastern China. JAMA Intern
333 Med. 2020; 180(12):1665-1671. doi: 10.1001/jamainternmed.2020.5225.
334 5. World Health Organization [WHO]. Modes of transmission of virus causing COVID-19:
335 implications for IPC precaution recommendations. 2020 [cited 2021 Jan 21].
336 https://www.who.int/news-room/commentaries/detail/modes-of-transmission-of-virus-
337 causing-covid-19-implications-for-ipc-precaution-recommendations.
338 6. Atkinson J, Chartier Y, Pessoa-Silva CL, Jensen P, Li Y, Seto W-H. Natural Ventilation for
339 Infection Control in Health-Care Settings. World Health Organization: Geneva, Switzerland.
340 2009 [cited 2021 Jan 21].

https://apps.who.int/iris/bitstream/handle/10665/44167/9789241547857_eng.pdf;jsessionid=1A17F4B41AC402C2746778937A854E27?sequence=1.

7. Stadnytskyi V, Bax CE, Bax A, Anfinrud P. The airborne lifetime of small speech droplets and their potential importance to SARS-CoV-2 transmission. PNAS. 2020; 117(22):11875-11877. doi: 10.1073/pnas.2006874117.
8. Qian H, Miao T, Liu L, Zheng X, Luo D, Li Y. Indoor transmission of SARS-CoV-2. Indoor Air. 2020;00:1-7. doi: 10.1111/ina.12766.
9. Leclerc QJ, Fuller NM, Knight LE, Funk S, Knight GM. What settings have been linked to SARS-CoV-2 transmission clusters? Wellcome Open Res. 2020;5:83. doi: 10.12688/wellcomeopenres.15889.2.
10. Park S, Kim Y, Yi S, Lee S, Na B, Kim C, et al. Coronavirus disease outbreak in call center, South Korea. Emerg Infect Dis. 2020;26(8):1666-1670. doi: 10.3201/eid2608.201274.
11. van Doremalen N, Bushmaker T, Morris DH, Holbrook MG, Williamson BN, Tamin A, et al. Aerosol and surface stability of SARS-CoV-2 as compared with SARS-CoV-1. N Engl J Med. 2020;2020(382):1564-1567. doi: 10.1056/NEJMc2004973.
12. Chia PY, Coleman KK, Tan YK, Ong SWX, Gum M, Lau SK, et al. Detection of air and surface contamination by SARS-CoV-2 in hospital rooms of infected patients. Nat Comm. 2020;11:2800. doi: 10.1038%2Fs41467-020-16670-2.
13. Guo Z-D, Wang Z-Y, Zhang S-F, Li X, Li L, Li C, et al. Aerosol and surface distribution of severe acute respiratory syndrome coronavirus 2 in hospital wards, Wuhan, China, 2020. Emerg Infect Dis. 2020;26(7):1583-1591. doi: 10.3201/eid2607.200885.

14. Santarpia JL, Rivera DN, Herrera V, Morwitzer NJ, Creager H, Santarpia GW, et al. Transmission potential of SARS-CoV-2 in viral shedding observed at the University of Nebraska Medical Center. 2020. Preprint at doi: 10.1101/2020.03.23.20039446.

15. Orenes-Piñero E, Baño F, Navas-Carrillo D, Moreno-Docón A, Marín M, Misiego R, et al. Evidences of SARS-CoV-2 virus air transmission indoors using several untouched surfaces. Sci Tot Environ. 2020;751:142317. doi: 10.1016/j.scitotenv.2020.142317.

16. MultiState. COVID-19 State and Local Policy Dashboard. https://www.multistate.us/research/covid/public. 2009 [cited 2021 Jan 21].

17. Chande A, Lee S, Harris M, Nguyen Q, Beckett SJ, Hilley T, et al. Real-time, interactive website for US-county-level COVID-19 event risk assessment. Nat Hum Behav. 2020;4:1313-1319. doi: 10.1038/s41562-020-01000-9.

18. Bhagat RK, Davies Wykes MS, Dalziel SB, Linden PF. Effects of ventilation on the indoor spread of COVID-19. J Fluid Dynam. 2020;903:F1. doi: 10.1017/jfm.2020.720.

19. Chen W, Zhang N, Wei J, Yen H, Li Y. Short-range airborne route dominates exposure of respiratory infection during close contact. Build & Environ. 2020;176:106859. doi: 10.1016/j.buildenv.2020.106859.

20. Lelieveld J, Helleis F, Borrmann S, Cheng Y, Drewnick F, Haug G, et al. Model calculations of aerosol transmission and infection risk of COVID-19 in indoor environments. Int J Environ Res Pub Health. 2020;17:8114. doi: 10.3390/ijerph17218114.

21. Miller SL, Nazaroff WW, Jimenez JL, Boerstra A, Buonanno G, Dancer SJ, et al. Transmission of SARS-CoV-2 by inhalation of respiratory aerosol in the Skagit Valley Chorale superspreading event. Indoor Air. 2020;00:1-10. doi: 10.1111/ina.12751.

384 22. Sun C, Zhai Z. The efficacy of social distance and ventilation effectiveness in preventing
385 COVID-19 transmission. Sust Cities Soc. 2020;62:102390. doi: 10.1016/j.scs.2020.102390.
386 23. Riley EC, Murphy G, Riley RL. Airborne spread of measles in a suburban elementary school.
387 Am J Epidem. 1978;107(5):421-432. doi: 10.1093/oxfordjournals.aje.a112560.
388 24. Shao S, Zhou D, He R, Li J, Zou S, Mallery K, et al. Risk assessment of airborne
389 transmission of COVID-19 by asymptomatic individuals under different practical settings. J
390 Aerosol Sci. 2021;151:105661. doi: 10.1016/j.jaerosci.2020.105661.
391 25. Wilensky U. NetLogo. Center for Connected Learning and Computer-Based Modeling,
392 Northwestern University, Evanston, IL. http://ccl.northwestern.edu/netlogo/. 1999 [cited
393 2021 Jan 21].
394 26. Grimm V, Railsback SF, Vincenot CE, Berger U, Gallagher C, DeAngelis DL, et al. The
395 ODD protocol for describing agent-based and other simulation models: a second update to
396 improve clarity, replication, and structural realism. J Artif Soc Soc Simul. 2020;23(2):7. doi:
397 10.18564/jasss.4259.
398 27. Adams WC. Measurement of breathing rate and volume in routinely performed daily
399 activities. 1993. Final Report, Contract No. A033-205. California Air Resources Board,
400 Sacramento, CA, USA.
401 https://ww2.arb.ca.gov/sites/default/files/classic//research/apr/past/a033-205.pdf.
402 28. Jefferson T, Foxlee R, Del Mar C, Dooley L, Ferroni E, Hewak B, et al. Physical
403 interventions to interrupt or reduce the spread of respiratory viruses: systematic review. BMJ.
404 2008;2008(336):77. doi: 10.1136/bmj.39393.510347.BE.

29. Asadi S, Cappa CD, Barreda S, Wexler AS, Bouvier NM, Ristenpart WD. Efficacy of masks and face coverings in controlling outward aerosol particle emission from expiratory activities. Sci Rep. 2020;10:15665. doi: 10.1038/s41598-020-72798-7.

30. O'kelly E, Pirog S, Ward J, Clarkson PJ. Ability of fabric face mask materials to filter ultrafine particles at coughing velocity. BMJ Open. 2020;10(9):e039424. http://dx.doi.org/10.1136/bmjopen-2020-039424.

31. Ferrari SLP, Cribari-Neto F. Beta regression for modelling rates and proportions. J Appl Stat. 2004;31(7): 799-815. doi: 10.1080/0266476042000214501.

32. Cribari-Neto F, Zeileis A. Beta regression in R. J Stat Soft. 2010;34(2):1-24. doi: 10.18637/jss.v034.i02.

33. Smithson M, Verkuilen J. A better lemon squeezer? Maximum-likelihood regression with beta-distributed dependent variables. Psych Methods. 2006;11(1):54-71. doi: 10.1037/1082-989x.11.1.54.

34. RStudio Team. RStudio: integrated development Environment for r. RStudio Team, Boston, Massachusetts, USA. http://www.rstudio.com. 2018 [cited 2021 Jan 21].

35. R Core Team. R: A language and environment for statistical computing. R Foundation for Statistical Computing, Vienna, Austria. https://www.R_project.org. 2020 [cited 2021 Jan 21].

36. Tjur, T. Coefficients of determination in logistic regression models – A new proposal: The coefficient of discrimination. Am Stat. 2009;63(4):366 – 372. doi: 10.1198/tast.2009.08210.

37. Agrawal A, Bhardwaj R. Reducing chances of COVID-19 infection by a cough cloud in a closed space. Phys Fluids 2020;32:101704. doi: 10.1063/5.0029186.

426 38. Escombe AR, Oeser CC, Gilman RH, Navincopa M, Ticona E, Pan W, et al. Natural
427 ventilation for the prevention of airborne contagion. PLoS Med. 2007;4(2):e68. doi:
428 10.1371/journal.pmed.0040068.
429 39. Smieszek T, Lazzari G, Salathé M. Assessing the dynamics and control of droplet- and
430 aerosol-transmitted influenza using an indoor positioning system. Sci Rep. 2019;9:2185. doi:
431 10.1038/s41598-019-38825-y.
432 40. Lee KK, Savani A, Matos S, Evans DH, Pavord ID, Birring SS. Four-hour cough frequency
433 monitoring in chronic cough. CHEST. 2012;142(5):1237-1243. doi: 10.1378/chest.11-3309.
434 41. Kwon S-B, Park J, Jang J, Cho Y, Park D-S, Kim C, et al. Study on the initial velocity
435 distribution of exhaled air from coughing and speaking. Chemosphere. 2012;87(11):1260-
436 1264. doi: 10.1016/j.chemosphere.2012.01.032.
437 42. Bourouiba L, Dehandschoewercker E, Bush JWM. Violent expiratory events: on coughing
438 and sneezing. J Fluid Mech. 2014;745(2014):537-563. doi: 10.1017/jfm.2014.88.
439 43. Das SK, Alam J, Plumari S, Greco V. Transmission of airborne virus through sneezed and
440 coughed droplets. Phys Fluids. 2020;32:097102. doi: 10.1063/5.0022859.
441 44. Fryar CD, Kruszon-Moran D, Gu Q, Ogden CL. Mean body weight, height, waist
442 circumference, and body mass index among adults: United States, 1999–2000 through 2015–
443 2016. National Health Statistics Reports, No. 122. United States National Center for Health
444 Statistics, Hyattsville, MD, USA. 2018. https://stacks.cdc.gov/view/cdc/61430.
445 45. Wölfel R, Corman VM, Guggemos W, Sailmaier M, Zange S, Müller MA, et al. Virological
446 assessment hospitalized patients with COVID-2019. Nature 2020;581(2020): 465-469. doi:
447 10.1038/s41586-020-2196-x.

448 46. Castillo JE, Weibel JA. A point sink superposition method for predicting droplet interaction
449 effects during vapor-diffusion-driven dropwise condensation in humid air. Int J Heat Mass
450 Trans. 2018;118(2018):708-719. doi: 10.1016/j.ijheatmasstransfer.2017.11.045.
451 47. Chao CYH, Wan MP, Morawska L, Johnson GR, Ritovski ZD, Hargreaves M, et al.
452 Characterization of expiration air jets and droplet size distributions immediately at the mouth
453 opening. J. Aerosol Sci. 2009;40(2):122-133. doi: 10.1016/j.jaerosci.2008.10.003.

454 **Tables**

455 Table 1. Parameter descriptions for simulations of the Skagit County, WA March 2020 SARS-
456 CoV-2 transmission case study.

Parameter/Model Input	Value(s)	Reference(s)
Infectiousness parameters		
Cough frequency (coughs/min)	0.19	*40*
Droplet count (droplets/expectoration)	$9.7e^5$ ($3.9e^5$)†	*21,* Appendix S2
Droplet spread angle – coughing (º)	35	*41*
Droplet spread angle – not coughing (º)	63.5	*41*
Droplet travel distance – coughing (m)	5 (0.256)†	*42*
Droplet travel distance – not coughing (m)	0.55 (0.068)†§	*43*
Scenario environment and individual behavior inputs		
Area (m^2)	180*	*2*
Expectoration height (m)	1.7	*44*
Inhalation rate (m^3 air/min)	0.023	*27*

Maximum people in a single 1-m^2 patch (people)	2	*2*
Number of symptomatic individuals (people)	1	*2*
Scenario virion behavior inputs		
Virion count (virions/mL fluid)	$2.35e^9$	*45*
Virion decay rate (%/min)	1.05	*11*
Virion infection risk (%/inhaled virion)	6.24	Appendix S2
Scenario airflow inputs		
Diffusion rate (m^3/min)	$1.5e^{-3}$	*46*
Forced air	on, off	–
Forced air direction	North-to-South, East-to-West	–
Air change rate (%/min)	4.3	*21*
Re-circulated air filtration (%/min)	90	*21*
Scenario intervention inputs		
Attempted social distancing (m)	0, 1, 2, 3	–
Contact duration (min)	20, 40, 60, 90, 105, 150	–
Mask efficacy (%)	0‡, 25, 50, 75, 90	*28, 29*
Population (people)	10, 50, 61	*2, 16*

*Simulated worlds were 10 m X 18 m. †Standard deviations are given in parentheses. ‡Zero-percent mask efficacy is equivalent to no mask use. §Das et al. (2020) (*45*) estimated the average travel distance of a 100-micrometer droplet expelled from a height of 1.7 m at a velocity of 0.5 m/s to be 0.55 m. They also found that the majority of 100-µm droplets will fall 0.55-2.35 m

461 away from the expelling individual, depending on initial velocity, but droplets may settle up to
462 3.2 m away very rarely. a random draw of 10,000,000 samples from a log-normal distribution
463 parameterized using 1.7-m and 0.2095-m droplet spread distance mean and standard deviation
464 values, respectively, generated a distribution in line with this finding. The standard deviation we
465 use in simulations for non-coughing expectoration is proportionate to the one used in this random
466 draw.
467
468 Table 2. Parameter descriptions for ventilation-system effect evaluations.

Parameter/Model Input	Value(s)	Reference(s)
Infectiousness parameters		
Cough frequency (coughs/min)	0.19	*40*
Droplet count (droplets/expectoration)†	1,000 (0)‡, $9.7e^5$ ($3.9e^5$)‡	*21,* Appendix S2
Droplet spread angle – coughing (º)	35	*41*
Droplet spread angle – not coughing (º)	63.5	*41*
Droplet travel distance – coughing (m)	5 (0.256)‡	*42*
Droplet travel distance – not coughing (m)	0.55 (0.068)‡§	*43*
Scenario environment and individual behavior inputs		
Area (m^2)*	9, 36, 81	–
Expectoration height (m)	1.7	*44*
Inhalation rate (m^3 air/min)	0.023	*27*
Maximum people in a single 1-m^2 patch (people)	2	*2*
Number of infectious individuals (people)	1	–

Proportion of infectious individuals that are symptomatic (%)	0, 100	–
Scenario virion behavior inputs		
Virion count (virions/mL fluid)	$2.35e^{9}$	*45*
Virion decay rate (%/min)	1.05, 5¶, 10¶, 25¶, 50¶, 75¶, 90¶	*11*
Virion infection risk (%/inhaled virion)	6.24	Appendix S2
Scenario airflow inputs		
Diffusion rate (m^3/min)	$1.5e^{-3}$	*46*
Forced air	on, off	–
Forced air direction**	East-to-West	–
Air change rate (%/min)	0#, 1¶, 5¶, 10¶, 25¶, 50¶	–
Re-circulated air filtration (%/min)	0#,1¶, 5¶, 90¶, 100¶	–
Scenario intervention inputs		
Attempted social distancing (m)	0	–
Contact duration (min)	10, 30, 60	–
Mask efficacy (%)	0††	–
Population density (people/m^2)‡‡	0.333, 0.667, 1, 1.667	–

*All simulated worlds were square-shaped. †Based on linear modeling described in Appendix S2, these values equate to 1 (SD = 0) and 970 (SD = 390) quanta/hr. ‡Standard deviations are given in parentheses. §Das et al. (2020) (*45*) estimated the average travel distance of a 100-micrometer droplet expelled from a height of 1.7 m at a velocity of 0.5 m/s to be 0.55 m. They also found

that the majority of 100-µm droplets will fall 0.55-2.35 m away from the expelling individual, depending on initial velocity, but droplets may settle up to 3.2 m away very rarely. a random draw of 10,000,000 samples from a log-normal distribution parameterized using 1.7-m and 0.2095-m droplet spread distance mean and standard deviation values, respectively, generated a distribution in line with this finding. The standard deviation we use in simulations for non-coughing expectoration is proportionate to the one used in this random draw. ¶These parameter values were only used when the "Forced air" parameter value was set to "on." #These parameter values were only used when the "Forced air" parameter value was set to "off." **All patches on the east side of the simulated world acted as supply vents. All patches on the west side acted as return vents. ††Zero-percent mask efficacy is equivalent to no mask use. ‡‡Instead of specifying a fixed number of individuals in simulations, we scaled the simulated population with world size.

Table 3. Logit scale estimates associated with 1-unit increases in covariate values given by our beta-regression model for evaluating intervention effects. Wald 95% confidence intervals are given in parentheses.

Coefficient	Estimate	*p*
Intercept	-2.927 (-2.940, -2.914)	–
ϕ	5.808 (5.791, 5.824)	–
Gathering duration (min)	0.012 (0.012, 0.012)	< 0.001
Mask efficacy (%)	-0.015 (-0. 015, -0.015)	< 0.001
Mask use	-0.949 (-0.964, -0.935)	< 0.001
Movement (No. rearrangements)	0.491 (0.485, 0.497)	< 0.001
Group size (people)	0.001 (0.001, 0.001)	< 0.001

Social distancing (m)	-0.250 (-0.256, -0.243)	< 0.001
Ventilation	0.898 (0.895, 0.902)	< 0.001
Mask use : **Group size**	0.014 (0.013, 0.014)	< 0.001
Mask use : **Social distancing**	-0.018 (-0.025, -0.010)	< 0.001
Group size : **Social distancing**	0.004 (0.004, 0.004)	< 0.001
Mask use : **Group size** : **Social distancing**	$1.923e^{-4}$ ($3.039e^{-5}$, $3.542e^{-4}$)	0.020

Table 4. Logit scale estimates associated with 1-unit increases in covariate values given by our logistic-regression model for evaluating effect on SARS-CoV-2 transmission risk during an indoor gathering. Wald 95% confidence intervals are given in parentheses.

Coefficient	Estimate	Odds ratio	*p*
Intercept	-0.146 (-0.151, -0.140)	–	–
Population density (people/m^2)	2.766 (2.761, 2.771)	15.891 (15.813, 15.968)	< 0.001
Gathering duration (min)	0.015 (0.015, 0.015)	1.015 (1.015, 1.015)	< 0.001
Quanta (quanta/hr)	0.002 (0.002, 0.002)	1.002 (1.002, 1.002)	< 0.001
Excess droplet removal rate (%/min)	-0.024 (-0.024, -0.024)	0.976 (0.976, 0.976)	< 0.001
Air change rate (%/min)	0.017 (0.017, 0.017)	1.02 (1.02, 1.02)	< 0.001
Air filtration rate (%/min)	-0.005 (-0.005, -0.005)	0.995 (0.995, 0.995)	< 0.001

Figures

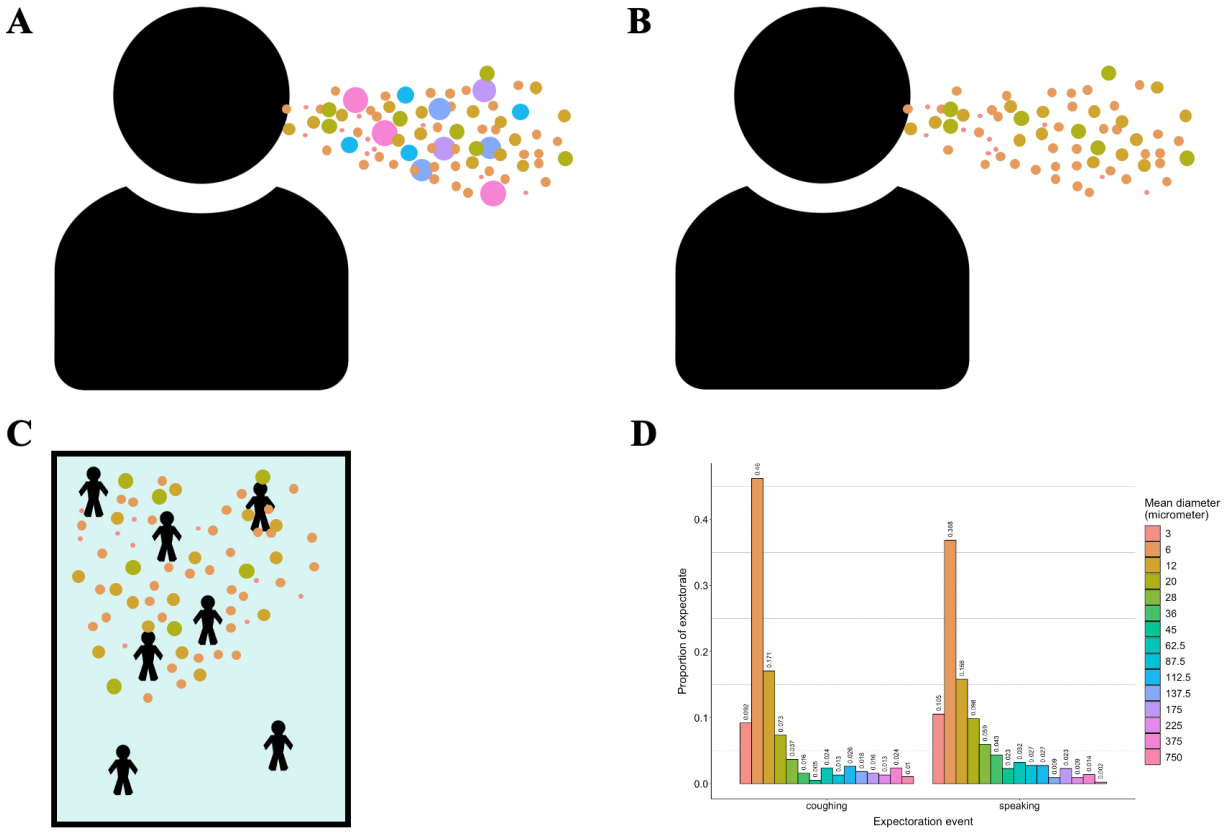

Figure 1. Model droplet dynamics. A) Infectious individuals expel droplets of different sizes. B) Relatively large droplets fall out of the air quickly post expectoration. C) Smaller droplets remain aerosolized for longer time periods and move throughout the simulated room via diffusion and forced airflow effects. D) Distribution of droplet sizes during expectoration events. Distributions of size classes during coughing and speaking events are based on findings of (*47*), and represent mean observed droplet-size measurements they recorded 60 mm away from individuals' mouths immediately following these activities.

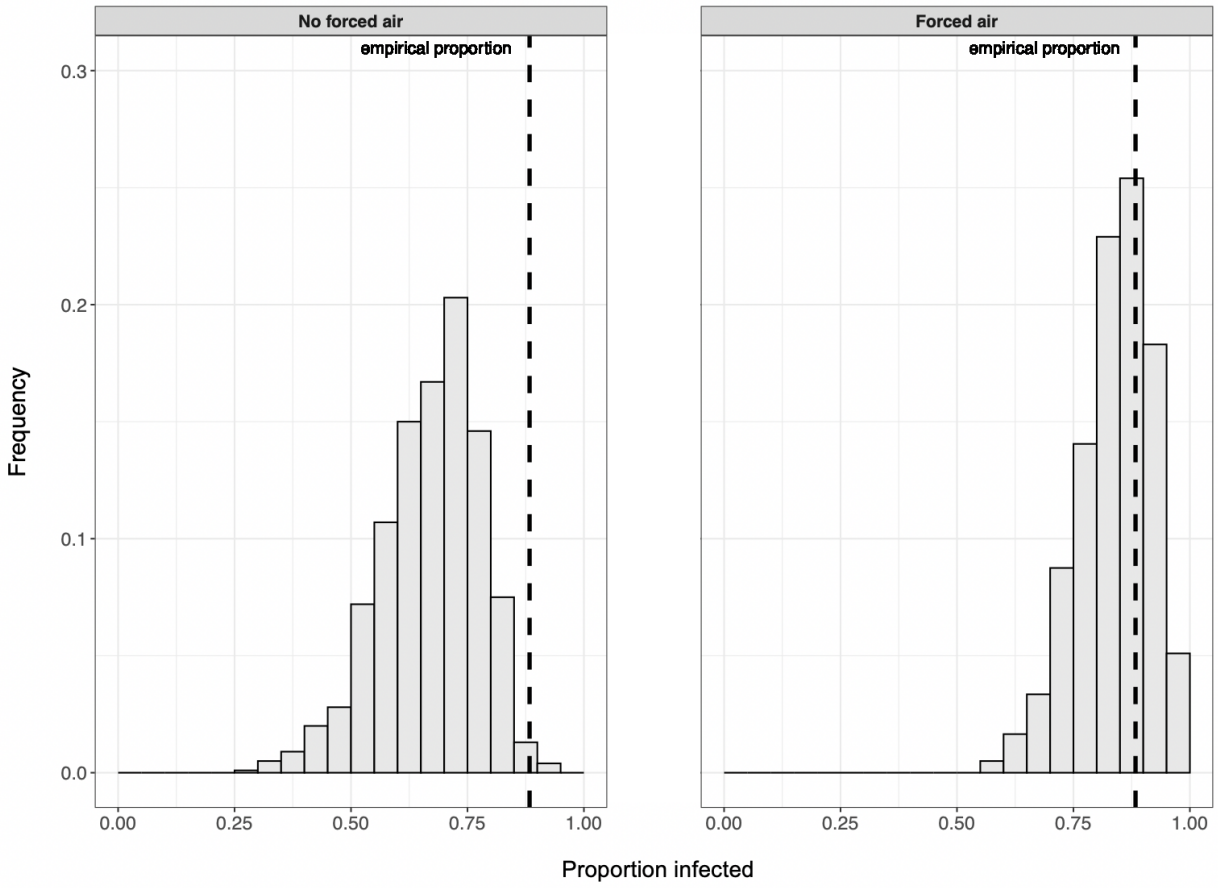

503

504 Figure 2. In the absence of interventions to reduce transmission risk, the proportion of

505 susceptible people infected in simulations can reflect the case study value (i.e., 0.88) and is more

506 likely to do so when forced airflow is included.

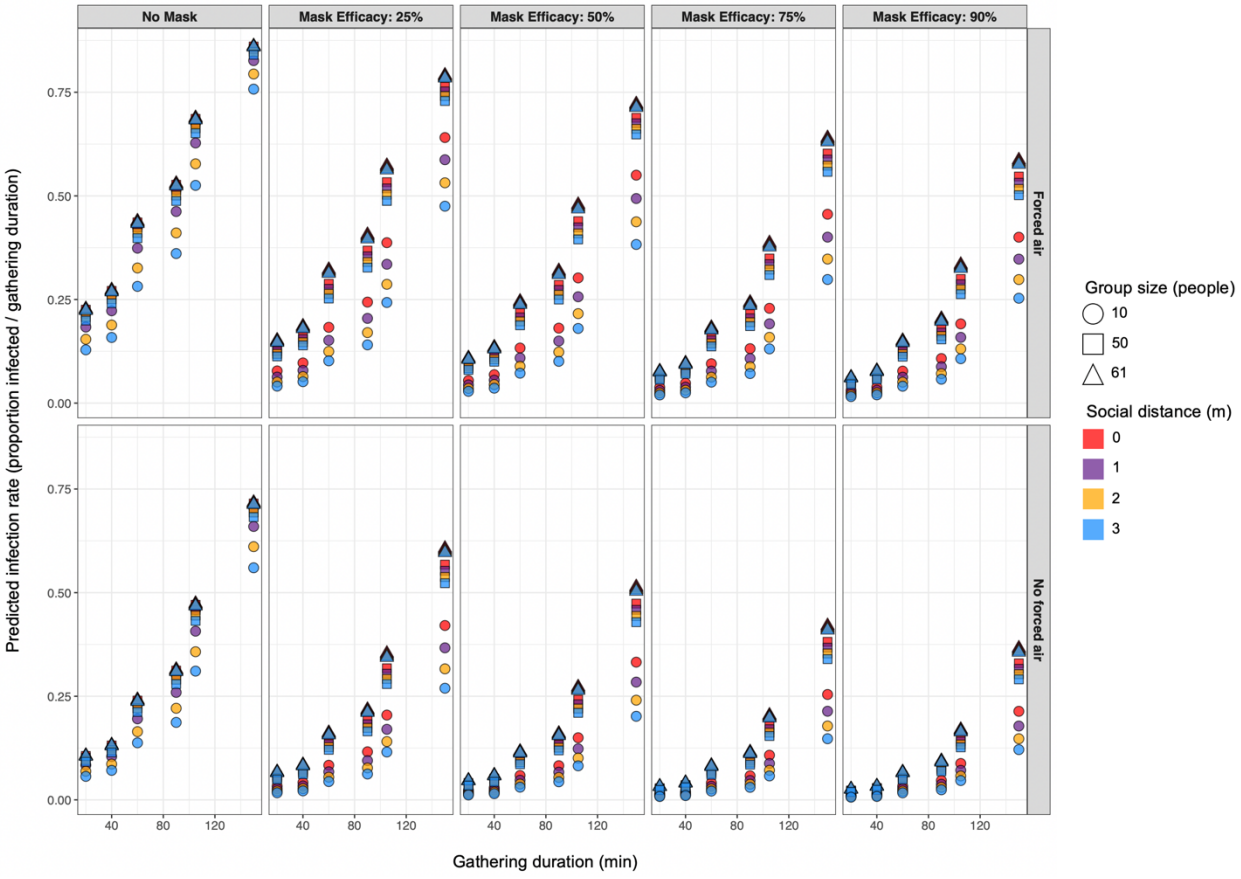

Figure 3. Predicted proportion of susceptible populations infected with SARS-CoV-2 for varied parameter sets suggest that concurrent deployment of multiple interventions is required to achieve near-zero transmission rates.